Analysis of Separation Control by Means of Tangential Blowing

E. S. Levinsky* and R. H. Schappelle†
Convair Division of General Dynamics, San Diego, Calif.

A computational procedure is described for predicting the critical jet momentum coefficient for achieving full potential lift by means of tangential blowing on airfoils with unslotted flaps. Among the applications of the procedure are the design and optimization of tangential blowing BLC systems for advanced fighter and transport type STOL aircraft and for over-the-wing blowing. The procedure incorporates a velocity profile with a velocity minimum, due to upstream boundary-layer and slot lip thickness effects, to describe the jet layer; and the initial jet velocity profile downstream of the slot exit contains an inviscid core region with a maximum velocity based on the total pressure inside the slot, rather than on empirical assumptions.[1] The procedure utilizes the strip-integral technique to reduce the partial differential equations describing the jet layer flow to ordinary differential equations, and assumptions are made regarding the turbulent shear stress values at the boundaries and midpoints of each strip in order to carry out the integration. Computer programming of the procedure has been carried out, and a limited number of comparisons showing reasonably good agreement between the computational procedure and test results are shown.

Nomenclature

$A_q, B_q, \ldots H_q$ = coefficients defined in Appendix for $q = 1, 2, \ldots 7$
C_L = lift coefficient
C_μ = jet momentum coefficient
c = chord length
c_f = local skin friction coefficient
c_p = local pressure coefficient
$F_{31}, F_{\frac{3}{2}1}, \ldots F^*_{\frac{4}{2}2}$ = integrals defined in Appendix
f, g = similarity functions defined in Figs. 3 and 4, respectively
n = exponent in power law boundary layer profile (Eq. 1)
p = static pressure
R = radius of curvature
R_T* = turbulent Reynolds number in outer part of boundary layer
s = slot edge thickness, also arc length along airfoil
t = slot width
u, v = tangential and normal velocity components
V_∞ = remote freestream velocity
x, y = coordinates parallel and normal to the surface
$y_{1/2}$ = mid velocity point in wake zone defined in Fig. 1
α = angle of attack
δ = boundary-layer thickness
$\delta_1, \ldots \delta_3$ = heights above surface of various zones depicted in Fig. 1
δ_f = trailing flap deflection angle
δ_n = nose flap deflection angle
$\Delta\tau_q$ = difference in turbulent shear stress defined in Table 2 for $q = 1, 2, \ldots 7$
η_3, η_4 = nondimensional distances in jet and wake zones depicted in Figs. 3 and 4
$\bar{\eta}_3$ = nondimensional distance to mid velocity point in jet zone defined in Figs. 1 and 3
ν = kinematic viscosity
ν_t = effective eddy viscosity
ρ = mass density
τ = turbulent shear stress

Subscripts

e = local conditions just outside viscous regions
j = jet
m = maximum value
w = minimum wave
$CRIT$ = critical value
∞ = remote freestream value

Superscripts

$'$ = lower boundary-layer inside slot, also $d/d\eta_3$ and $d/d\eta_4$
$''$ = upper boundary-layer inside slot
$'''$ = outside boundary-layer just upstream of slot exit

Received February 11, 1974; revision received July 29, 1974.
Index categories: Aircraft Aerodynamics (Including Component Aerodynamics); Jets, Wakes, and Viscid-Inviscid Flow Interactions.

*Staff Scientist, Aerodynamics. Member AIAA.
†Senior Research Engineer, Design Analysis Programing.

I. Introduction

ALTHOUGH it is well known that increased take off and landing performance may be obtained with tangential blowing BLC systems, a reliable analytical procedure for designing and optimizing a tangential blowing system for a specific aircraft and engine combination is currently not available. Such a procedure should include effects of slot geometry (slot height and lip thickness), slot location, airfoil shape, and scale. An analytical procedure of this type should also be useful for extrapolating to full scale wind tunnel data obtained on small scale models, and for evaluating competitive BLC systems, e.g. spanwise blowing over trailing flaps[2] and spanwise blowing in the vicinity of the leading edge.

Many procedures have been developed for estimating the critical value of jet momentum coefficient required to move the separation point on an airfoil or flap surface to the trailing edge and thereby to obtain full potential lift. Among such methods are those by Thomas[3] and Carriere and Eichelbrenner.[4] A method was also developed by the first of the present authors in connection with turbulent Coanda jet calculations.[1] Although these methods presently may be used to estimate the critical jet momentum coefficient, they require the introduction of many simplifying assumptions and empirical relations, and any agreement with test results may be fortuitous. A reason for the lack of any general procedure for tangential blowing is due to the difficulty of analytically modeling the complicated turbulent mixing process which occurs in the jet layer, especially just downstream of the slot exit and near the separation point. The problem is even more difficult than that encountered in predicting the growth and separation of a turbulent boundary layer (e.g., Ref. 5), because of the complex nature of the velocity distribution across the jet layer, and because of the lack of extensive test data relating to the distribution of velocity and shear stress in the layer.

In the present paper an analytical method is formulated for predicting the development, decay, and separation of an incompressible, two-dimensional, turbulent jet over

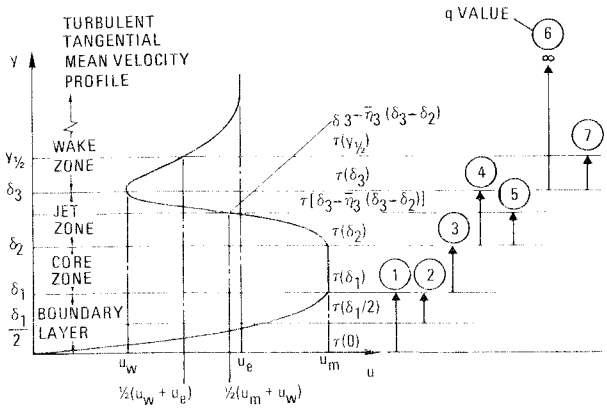

Fig. 1 Zones in jet layer for multi-strip integral method.

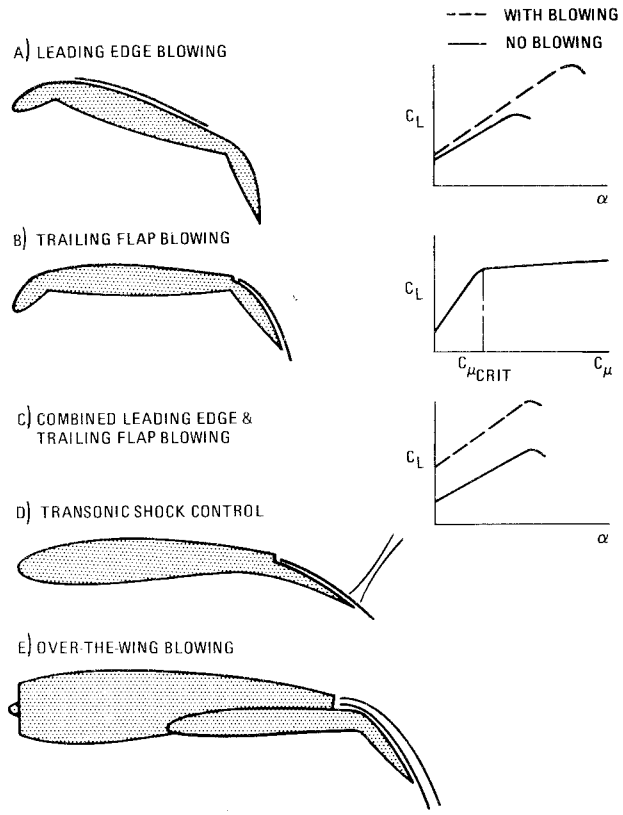

Fig. 2 Applications of tangential blowing separation control.

the surface of an airfoil or flap. The method, which utilizes the multistrip integral approach to solve the momentum integral equation, is an extension of the approach previously presented in Ref. 1. The current method utilizes a more general velocity profile with a velocity minimum. This velocity minimum, which is caused by the external boundary layer ahead of the jet slot and by the internal boundary layer inside the jet nozzle and by the nozzle lip thickness, is believed to exert a large influence on the subsequent jet development and separation, as indicated in Ref. 1. In addition, the velocity profile in the current method is assumed to start with an inviscid core region just downstream of the jet exit (see Fig. 1). The maximum velocity in the core region is based on the total pressure inside the slot, and hence no empirical assumption is required for the initial value of the maximum velocity, as was the case in Ref. 1. The decay and disappearance of the core region is predicted by the method, in addition to the growth and separation of the jet both prior and subsequent to the disappearance of the core region.

In the present formulation, the jet is subdivided into four layers (or zones): a wall boundary layer, an inviscid core zone, a jet layer, and a wake layer with a velocity minimum (Fig. 1). The velocity profile across each layer is assumed to be given by a separate similarity function based on test results. In addition to specification of these similarity distributions, the method requires that the turbulent shear stress be defined in terms of the velocity profile parameters at the edges and midpoints of each zone.

By means of the multistrip integral approach, the problem has been reduced to the stepwise integration of seven ordinary differential equations for seven parameters which are used to define the velocity profile. The inviscid pressure distribution is assumed to be known, and starting conditions for the velocity profile parameters are obtained from the upstream boundary layer and jet characteristics. The integration is terminated when a criterion for turbulent separation is met.

The method may be applied to a variety of flows in which tangential blowing is used to reduce or eliminate flow separation, e.g., leading edge BLC, trailing flap BLC, and augmentor wing BLC. The method may also be used for configurations with thick jets and/or surfaces of large curvature, e.g., over the wing (OTW) blowing, provided variations in static pressure across the jet layer are included in the analysis.[1] Several possible applications for the method are illustrated in Fig. 2.

For each of these applications several trial calculations must usually be carried out, each with a different value of the jet momentum coefficient C_μ. The jet momentum is allowed to vary until the predicted separation point has moved to the trailing edge. The resulting value of the jet momentum coefficient is taken as the critical value $C_{\mu(CRIT)}$ for which full potential flow‡ is achieved. To simplify the procedure, the pressure distribution is assumed invariant with C_μ and is taken as that for full potential flow, even when separation does not occur at the trailing edge. Thus, the trial solutions are not compatible with the physical pressure distributions, except when $C_\mu = C_{\mu(CRIT)}$.

The method may be used to obtain effects of airfoil, flap, and slot geometry and slot chordwise position on $C_{\mu(CRIT)}$. The same method may also be used for three-dimensional effects provided that spanwise flow effects are negligible. This condition is generally met on moderate to high aspect ratio configurations for which lifting line theory may be employed to relate the two-dimensional and three-dimensional pressure distributions.

It should be recognized that the present method suffers from the well known limitations of integral and strip integral methods in that the shape of the velocity profiles must be assumed for each strip, and empirical expression must be used for the shear stresses at the edges and midpoints of the strips. Nevertheless, the method should prove useful for engineering estimates of $C_{\mu(CRIT)}$, even in comparison with finite difference approaches, as in Dvorak,[9] because of its relative simplicity and short computational time (approximately 1 min of CDC 6400 time per complete calculation for $C_{\mu(CRIT)}$). On the other hand,

‡Full potential flow as designated herein signifies a potential flow solution with the circulation chosen to satisfy the Kutta condition at the trailing edge. Potential flow pressure distributions are also possible for alternative trailing edge conditions, viz., flows with free streamline-type separation as discussed in Ref. 6 ($C_\mu < C_{\mu(CRIT)}$), and flows with supercirculation ($C_\mu > C_{\mu(CRIT)}$). The trial solutions could be made more compatible with the physical pressure distributions, when $C_\mu < C_{\mu(CRIT)}$, by calculating pressure distribution from a freestream line flow with the corresponding separation point according to Ref. 6. A similar extension to $C_\mu > C_{\mu CRIT}$ would require that the pressure distributions correspond to flows with supercirculation.[7,8]

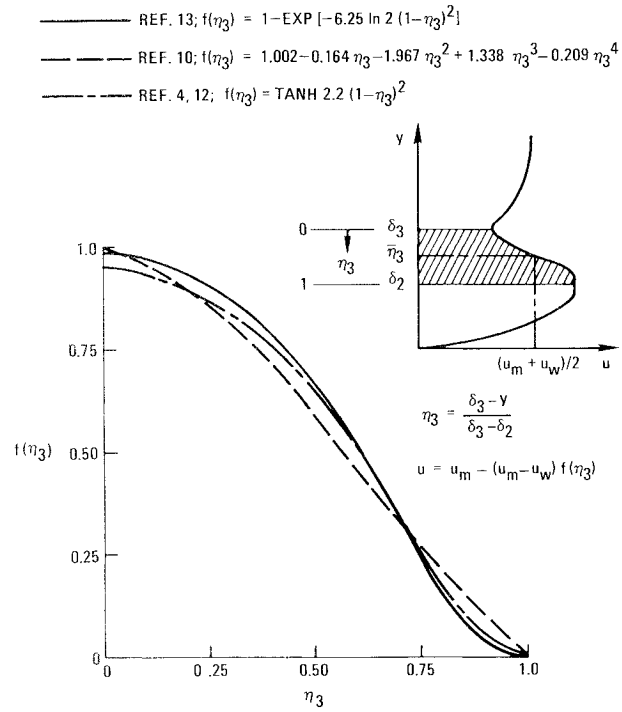

Fig. 3 Comparison of similarity distributions for velocity in wake zones, q = 4 and 5.

empirical assumptions pertaining to the representation of the Reynolds stress terms by an eddy viscosity model are still required in the finite difference approaches.

In Sec. II the multistrip integral procedure is formulated for the jet layer analysis, and expressions are given for the turbulent shear stress values. A discussion of the initial conditions and of the numerical integration procedure and separation criteria is given in Sec. III. Results of sample calculations and comparisons with test results are given in Sec. IV. Expressions for the coefficients in the strip-integral equations are listed in the Appendix.

II. Multi-Strip Integral Method for Tangential Blowing

A. Velocity Distribution

For application of the multistrip integral method to the tangential blowing problem the jet layer will be divided into four zones as depicted in Fig. 1, viz.

boundary layer	$0 \leq y \leq \delta_1$
core zone	$\delta_1 \leq y \leq \delta_2$
jet zone	$\delta_2 \leq y \leq \delta_3$
wake zone	$\delta_3 \leq y < \infty$

The horizontal component of velocity in each of these four zones will be assumed given in terms of experimentally determined similarity distributions involving the parameters n, u_m, u_w, u_e and $y_{1/2}$ in addition to δ_1, δ_2, and δ_3. Here n is an exponent used in the power law representation of the boundary layer, u_m is the maximum velocity in the profile, u_w is the minimum velocity, u_e is the free-stream velocity, and $y_{1/2}$ is the distance from the surface where the velocity attains the mean value between u_w and u_e. The parameters, except for u_e, are taken as unknowns which are allowed to vary with distance x from the slot and are to be determined as part of the solution. The velocity similarity profiles across the several zones are given by the following expressions:

boundary layer: $$u = u_m(y/\delta_1)^n \quad (1)$$

core zone: $$u = u_m \quad (2)$$

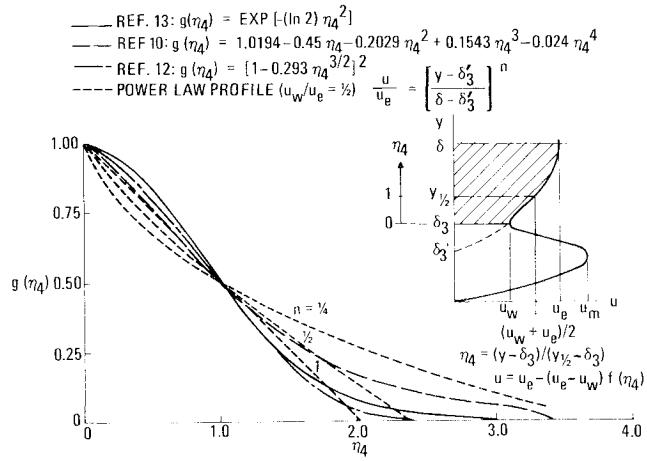

Fig. 4 Comparison of similarity distributions for velocity in wake zones, q = 6 and 7.

jet zone: $$u = u_m - (u_m - u_w)f(\eta_3) \quad (3)$$

wake zone: $$u = u_e - (u_e - u_w)g(\eta_4) \quad (4)$$

where

$$\eta_3 = (\delta_3 - y)/(\delta_3 - \delta_2),\ \eta_4 = (y - \delta_3)(y_{1/2} - \delta_3),$$

and where $f(\eta_3)$ and $g(\eta_4)$ are the similarity functions for the velocity distributions in the jet and wake zones, respectively.

The multistrip integral method may be derived formally without specification of the functional forms $f(\eta_3)$ and $g(\eta_4)$. Nevertheless, it is of interest to compare the functions $f(\eta_3)$ and $g(\eta_4)$, when based on data from tangential blowing wind tunnel tests,[10] with the functions from self-similar jet and wake analyses.[4,11-13] Comparisons of this type are shown in Figs. 3 and 4, and indicate that the self-similar distributions are reasonably close to the distributions obtained from the tangential blowing test data of Ref. 10. Nevertheless, it should be recognized that the data from Ref. 10 represent only a limited range of parameter variations, and additional test results are required to substantiate the similarity assumptions made in the analysis.

B. Differential Equations

We begin with the momentum integral equation between any two zones (or sub-zones) y_i and y_j, which may be written

$$2\int_{y_i}^{y_j} u\frac{\partial u}{\partial x}dy - u_j\int_{o}^{y_j}\frac{\partial u}{\partial x}dy + u_i\int_{o}^{y_i}\frac{\partial u}{\partial x}dy - u_e\frac{du_e}{dx}(y_j - y_i)$$

$$-\frac{\tau_j - \tau_i}{\rho} = -\int_{y_i}^{y_j}\frac{uv}{R}dy - \int_{y_i}^{y_j}\left[\frac{\partial(p/\rho)}{\partial x} + u_e\frac{du_e}{dx}\right]dy \quad (5)$$

Here the vertical velocity component v has been eliminated from the left-hand side of Eq. (5) through use of the continuity equation, and τ is the turbulent shear stress at the edge of the zone. The terms on the right-hand side include effects of streamline curvature and of static pressure variations across the zones as induced by surface curvature and separation. The right-hand side terms are of the order δ/R compared to the terms on the left-hand side, where R is the local radius of curvature. Hence, these terms will only be of importance for surfaces with sharp curvature. In order not to complicate the present formulation, and because the incorporation of the right hand side terms into the present formulation would be accomplished by a method similar to that described in Ref. 1 with simplified velocity profiles, the curvature terms will not be evaluated herein.

Table 1 Definition of independent strips

q	y_i	y_j
1	0	δ_1
2	$\delta_1/2$	δ_2
3	δ_1	δ_2
4	δ_2	δ_3
5	δ_2	δ_3-$\bar{\eta}_3(\delta_3 - \delta_2)$
6	δ_3	∞
7	δ_3	$y_{1/2}$

Restricting the formulation to the left-hand side of Eq. (5) and substituting therein Eqs. (1-4) for u gives, after some rearrangement, a set of ordinary differential equations of the form

$$A_q\frac{du_e}{dx} + B_q\frac{du_m}{dx} + C_q\frac{du_w}{dx} + D_q\frac{d\delta_1}{dx} + E_q\frac{dn}{dx} + F_q\frac{d\delta_2}{dx} + G_q\frac{d\delta_3}{dx} + H_q\frac{dy_{1/2}}{dx} - \frac{\Delta\tau_q}{\rho} = 0 \quad (6)$$

$$q = 1, 2, \ldots Q$$

where q identifies the particular strip and where the coefficients $A_q, \ldots H_q$ are algebraic functions of the dependent variables. Since u_e and $\Delta\tau_q$ are regarded as known, Eq. (6) must be evaluated for seven independent strips ($Q = 7$) prior to the disappearance of the core zone. For the present formulation the strips have been taken as defined in the Table 1, and the resultant coefficients A_q, B_q, etc., are as listed in the Appendix (Fig. 1).

Before the set of Eqs. (6) may be integrated step by step for the jet layer parameters, the turbulent shear stress differences $\Delta\tau_q$ across each strip must be known in terms of the jet layer parameters. In addition, initial values must be prescribed for the jet layer parameters just downstream of the jet exit, and the velocity distribution $u_e(x)$ must be known.

C. Turbulent Shear Stress Relations

The major assumptions in the multistrip integral method, or in any other method for turbulent flow, are connected with the determination of the turbulent shear stress values at distinct points inside the jet layer. The availability of only limited test data in this regard (e.g., Refs. 11, 12), and the complexity of the jet layer velocity profile in comparison with a boundary-layer profile, makes the evaluation of the shear stresses even more uncertain.

For the present formulation the shear stress at the wall $\tau(0)$ will be assumed given by the well-known Ludwig-Tillman law which may be expressed in the form

$$\left(\frac{V_\infty}{u_m}\right)^2\frac{c_f}{2} = \frac{\tau(0)}{\rho u_m^2} = 0.0128\left(\frac{\delta_1 u_m}{\nu}\right)^{-1/6}\times\left[\frac{n}{(n+1)(2n+1)}\right]^{(11n-1)/6} \quad (7)$$

At points inside the jet layer, the shear will be obtained by introducing an eddy viscosity term ν_t such that

$$\tau = \rho\nu_t(\partial u/\partial y) \quad (8)$$

Based on a logarithmic profile for the boundary-layer region and mixing length assumptions, it is readily shown that ν_t increases with distance from the wall according to the relation

$$\nu_t = 0.4u_m\delta_1(c_f/2)^{1/2}(y/\delta_1) \quad (9)$$

and reaches a maximum value

$$\nu_t = (n/n+1)(u_m\delta_1/R_T{}^*) \quad (10)$$

in the outer portion of the boundary layer, where for turbulent boundary layers, $R_T{}^* \sim 50$, e.g., Ref. 13. As also noted in Ref. 13, for wall jets $R_T{}^*$ decreases with increasing turbulence level in the jet layer. An empirical relation for $R_T{}^*$, derived by Gartshore and Newman[14] for self-preserving wall jets, is

$$R_T{}^* = 15 + 35\ exp\{-[\tau[\delta_3 - \bar{\eta}_3(\delta_3 - \delta_2)]/\tau_0]^2\} \quad (11)$$

and will be used in Eq. (10).

Thus, the shear stress at $\delta_1/2$ will be assumed given by the expression

$$\tau(\delta_1/2) = \left(\rho\nu_t\frac{\partial u}{\partial y}\right)_{\delta_1/2}$$

which for ν_t given by Eq. (10) becomes

$$\left(\frac{\tau}{\rho u_m{}^2}\right)_{\delta_1/2} = \frac{n^2}{(n+1)}\frac{2^{1-n}}{R_T{}^*} \quad (12)$$

The shear $\tau(\delta_1)$ is assumed equal to zero because the velocity gradient vanishes at the edge of the boundary layer. [$\tau(\delta_1)$ need not be zero for turbulent flow, because the velocity profile is not symmetrical about δ_1. However, test results show that τ changes sign very close to this location, hence the assumption $\tau(\delta_1) = 0$ is believed to be reasonably accurate.]

The eddy viscosity in the jet zone of Fig. 1 may be obtained from the free turbulent jet analysis given in Ref. 12. This gives

$$\nu_t = 0.037(u_m - u_w)(1 - \bar{\eta}_3)(\delta_3 - \delta_2) \quad (13)$$

where $f(\bar{\eta}_3) = 1/2$. The corresponding expression for the turbulent shear stress at the mid velocity point of the jet zone is

$$\tau[\delta_3 - \bar{\eta}_3(\delta_3 - \delta_2)] = 0.037(1 - \bar{\eta}_3)\rho(u_m - u_w)^2 f'(\bar{\eta}_3) \quad (14)$$

The shear stress at the edge of the wake zone $\tau(\delta_3)$ will be zero, since du/dy vanishes at that point.

For the outer wake region, the eddy viscosity will be based on a self-similar wake analysis (e.g., Ref. 12). This gives

$$\nu_t = 0.094(y_{1/2} - \delta_3)(u_e - u_w) \quad (15)$$

and the resulting shear stress becomes at $y = y_{1/2}$

$$\tau(y_{1/2}) = -0.094g'(\eta_4)_{\eta_4=1}\rho(u_e - u_w)^2 \quad (16)$$

The above relations enable the turbulent shear stress differences $\Delta\tau_q$ to be evaluated across each strip, as listed in Table 2.

III. Initial Conditions, Numerical Integration, and Separation Criterion

A. Initial Conditions

Initial values for the jet layer parameters just downstream of the slot exit will be obtained by fitting the simi-

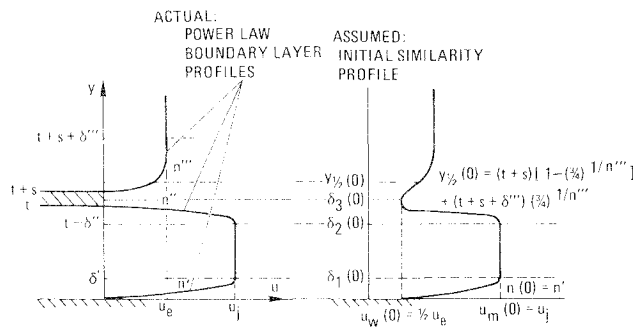

Fig. 5 Assumed initial conditions for similarity profile.

Table 2 Turbulent shear stress differences

q	$\Delta\tau_q$
1	$-\tau(0)$
2	$-\tau(\delta_1/2)$
3	0
4	0
5	$\tau[\delta_3 - \bar{\eta}_3(\delta_3 - \delta_2)]$
6	0
7	$\tau(y_{1/2})$

larity profiles for the various zones to the corresponding boundary layers just upstream of the slot. This initializing procedure is depicted in Fig. 5 where we take

$$u_m(0) = u_j$$

$$u_w(0) = 1/2\ u_e$$

$$n(0) = n'$$

$$\delta_1(0) = \delta'$$

$$\delta_2(0) = t - \delta''$$

$$\delta_3(0) = t + s/2$$

$$y_{1/2}(0) = (t + s)\left[1 - \left(\frac{3}{4}\right)^{1/n'''}\right] + (t + s + \delta''')\left(\frac{3}{4}\right)^{1/n'''}$$

and where the condition for $y_{1/2}(0)$ matches the mean velocity in the wake zone to that in the upstream boundary layer with a power law velocity profile at the same vertical height.

As noted from Fig. 5, the single primed terms represent the lower boundary layer inside the slot, the double primed terms represent the upper boundary layer inside the slot, and the triple primed terms refer to the outer boundary layer above the slot. The condition $u_w(0) = u_e/2$ is arbitrary, and was made to avoid the initial mixing region for which the assumption of similar velocity profiles must obviously fail. This condition may well require modification if the results prove highly sensitive to the value of $u_w(0)$.

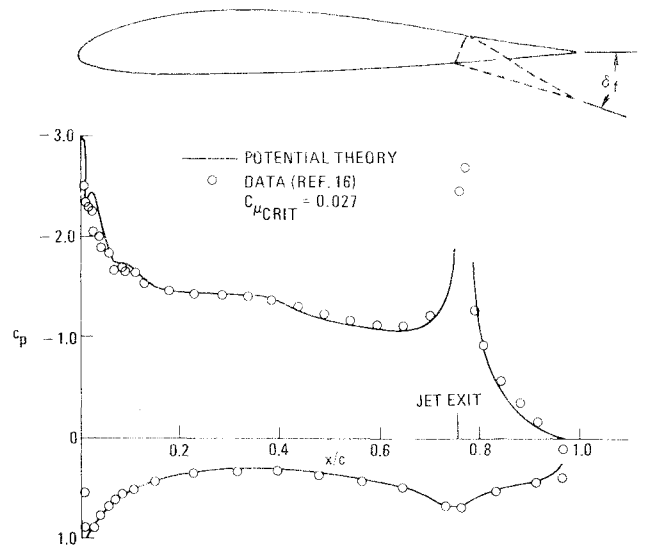

Fig. 6 Comparison of measured and calculated pressure distribution, case (1), $\alpha = 0°$, $\delta_n = 0°$, $\delta_f = 20°$.

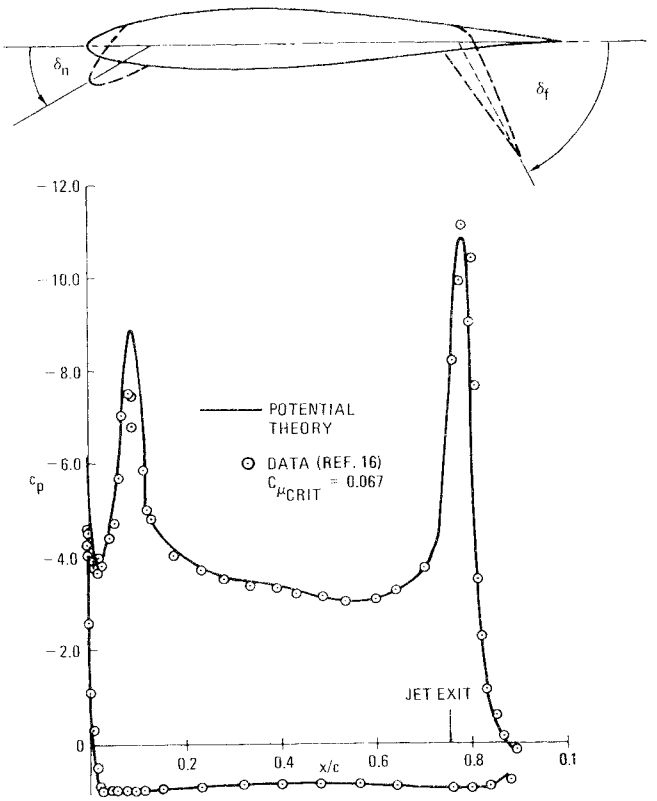

Fig. 7 Comparison of measured and calculated pressure distribution, case (2), $\alpha = 0°$, $\delta_n = 30°$, $\delta_f = 60°$.

B. Numerical Integration

A step-by-step integration procedure for the set of ordinary differential Eqs. (6), with the right-hand side curvature terms equated to zero, has been programed for the CDC 6400. The coefficients are as defined in Appendix A and the shear differences are as listed in Table 2. The integration is carried out with the four zone model until the core region vanishes, i.e., until $\delta_2 \leq \delta_1$. While the core region is present the equation for $q = 3$ links u_m to u_e according to the inviscid condition

$$u_m(du_m/dx) = u_e(du_e/dx)$$

Thus, the maximum velocity u_m in the jet is independent of any viscous effects. Once the core region vanishes, we set $\delta_1 = \delta_2$ and omit the equation for $q = 3$. In this case

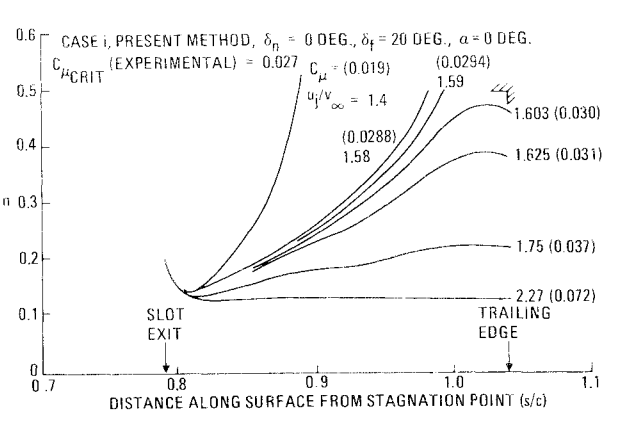

Fig. 8 Predicted effect of tangential blowing on jet layer exponent n, case (1).

the number of differential equations is reduced to six, and u_m is affected by viscous mixing.

The integration is to be carried out until the boundary-layer region satisfies a separation criterion. In general, several attempts are required to obtain the critical value of u_j, $u_j = u_{j(CRIT)}$, for which the separation point has been moved to the trailing edge of the airfoil. Thus, several values of u_j must be assumed for each case. As mentioned in the Introduction, the full potential flow pressure distribution is used for each assumed value of u_j. Hence, only the solution with $u_j = u_{j(CRIT)}$ is of physical significance.

Once $u_{j(CRIT)}$ has been established, the critical value of the jet momentum coefficient $C_{\mu(CRIT)}$ may be evaluated. Assuming incompressible flow, and accounting for viscous effects inside the slot

$$C_{\mu_{CRIT}} = 2\left(\frac{\rho_j}{\rho_\infty}\right)\left(\frac{u_j}{V_\infty}\right)_{CRIT}\left(\frac{u_{j\infty}}{V_\infty}\right)_{CRIT}\left(\frac{t}{c}\right)\times \left[1 - \frac{n''}{(n''+1)(2n''+1)}\left(\frac{\delta''}{t}\right) - \frac{n'}{(n'+1)(2n'+1)}\left(\frac{\delta'}{t}\right)\right] \quad (17)$$

where c is the reference chord, the subscript j refers to jet exit conditions, the subscript ∞ refers to freestream ambient conditions, and $u_{j(\infty)}$ is the velocity attained by the jet when expanded isentropically to ambient pressure. The term in square brackets in Eq. (17) accounts for the decrease in momentum flux due to the boundary layers inside the slot and was obtained by subtracting the momentum thickness of the interior boundary layers from the slot thickness. In terms of the local pressure coefficient $c_{p(j)}$ at the jet exit location

$$\left(\frac{u_{j\infty}}{V_\infty}\right)_{CRIT} = \left[\frac{\rho_\infty}{\rho_j}\,c_{P_j} + \left(\frac{u_j}{V_\infty}\right)^2_{CRIT}\right]^{1/2} \quad (18)$$

C. Separation Criterion

Various criteria for estimating turbulent boundary-layer separation have been proposed (e.g., Ref. 5). For the power-law-type boundary-layer profiles used in the present formulation, the condition

$$n = 1/2, \text{ with } dn/dx > 0 \text{ and } d^2n/dx^2 > 0 \quad (19)$$

will be used to locate the separation point.[1] An alternative condition from Ref. 5, for the case when n fails to reach $^1/_2$, is

$$dn/dx = 0$$

It is recognized that the Ludwig-Tillman law, Eq. (7), does not yield zero skin friction with $n = {}^1/_2$. Hence, the present separation criteria should be regarded as only approximate. An alternative formulation, utilizing a Coles law-of-the-wall and law-of-the-wake representation of the boundary-layer zone, and which includes a self-consistent expression for $\tau(0)$ which may become zero or even negative, could well result in improved estimates of separation.[15]

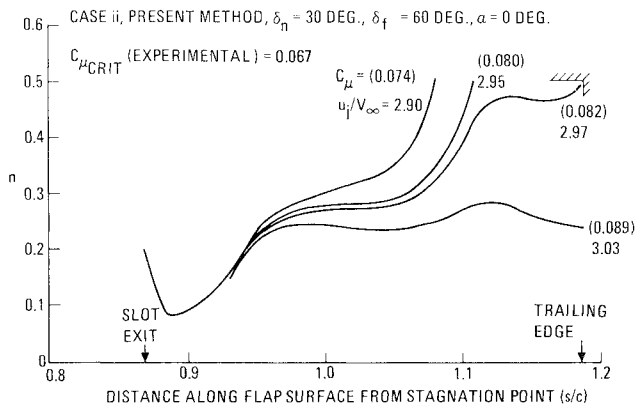

Fig. 9 Predicted effect of tangential blowing on jet layer exponent n, case (2).

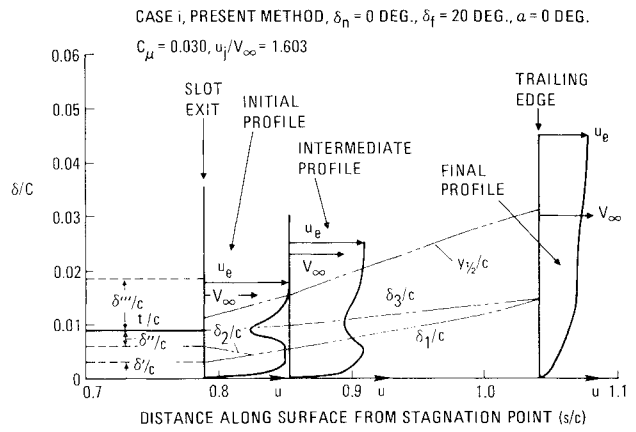

Fig. 10 Calculated jet layer growth and velocity profiles, case (1).

IV. Sample Calculations and Comparison with Test Data

Based on the tangential blowing method and computer program described in the previous sections, $C_{\mu(CRIT)}$ has been estimated for two cases. Calculations were made for the airfoil of Ref. 16 with a trailing edge flap deflection angle $\delta_f = 20°$, and a leading edge flap deflection angle $\delta_n = 30°$ together with $\delta_f = 60°$. The corresponding measured and calculated pressure distributions, along with the locations of the jet exit, are shown in Figs. 6 and 7, respectively. The test data were obtained with tangential blowing at the measured critical C_μ values of 0.027 and 0.067, respectively, and are closely approximated by the potential theory pressure distributions for these blowing coefficients. Thus, the assumption that the potential theory pressure distribution is valid at $C_{\mu(CRIT)}$ appears to have been substantiated, at least for the two test cases.

By carrying out jet layer calculations with various amounts of blowing, the variations of n vs x/c shown in Figs. 8 and 9 were obtained. In all cases, the initial values

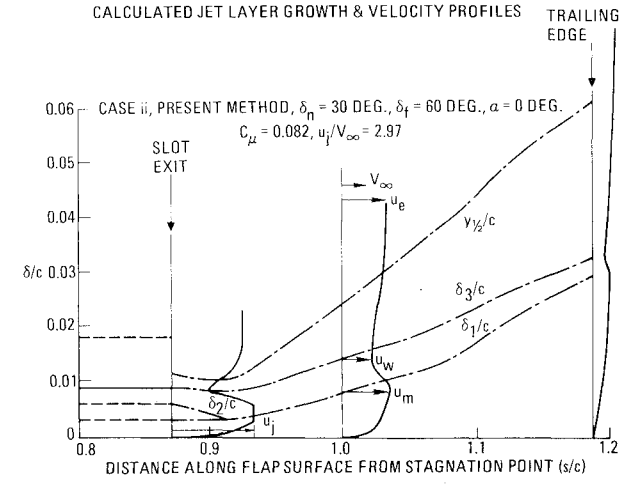

Fig. 11 Calculated jet layer growth and velocity profiles, case (2).

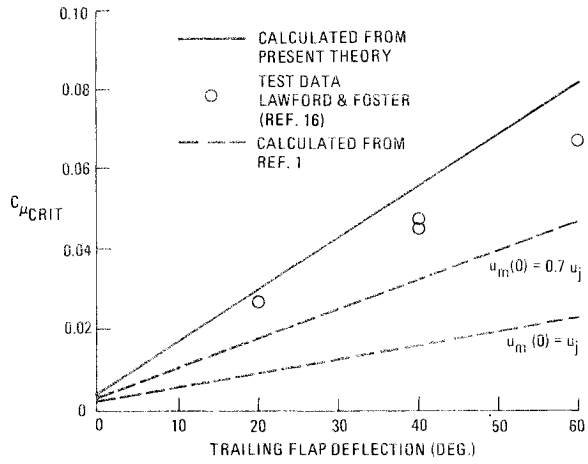

Fig. 12 Comparison between calculated and measured critical momentum coefficient for full BLC.

$$n' = n'' = n''' = 1/5$$

$$\delta' = \delta'' = t/3$$

and

$$\delta''' = 1.15t$$

were used. All jet layer calculations were made for the potential theory pressure distributions shown in Figs. 6 and 7, hence, as noted previously, only those jet layer calculations for $C_\mu = C_{\mu(CRIT)}$ are physically valid. As observed from Figs. 8 and 9, the calculated values of $C_{\mu(CRIT)}$ needed to move the separation point to the trailing edge are $C_{\mu(CRIT)} = 0.03$ and 0.082 for $\delta_f = 20°$ and 60°, respectively.

The calculated jet layer growth characteristics and velocity profiles for these two cases are illustrated in Figs. 10 and 11. (Vertical scales have been expanded by a factor of 2.5 for clarity). The disappearance of the inviscid core region and the gradual decay of the velocity maxima and minima in the jet layer profiles are clearly shown for both cases.

The calculated values of $C_{\mu(CRIT)}$ are compared with the test results versus δ_f in Fig. 12. Also shown in Fig. 12 are calculated values from Ref. 1 for two assumed values of $u_m(0)$. It is clear that the present method affords improved agreement with the test results in comparison with Ref. 1 and does not require any assumption concerning $u_m(0)$. Nevertheless, further comparisons with test data covering a wider range of geometric parameters, e.g. slot height, lip thickness, slot chordwise location, flap chord, etc., and a range of Reynolds numbers are required to substantiate the method as a general computational procedure.

V. Conclusions

A computational method and computer program have been developed for estimating the tangential blowing requirements for achieving full potential flow on airfoils with plain leading edge and trailing edge flaps. The method has been shown to compare favorably with test data for two flap deflection angles.

In order to establish the generality of the method, it is recommended that additional comparisons with test data be carried out over a wider range of geometric parameters and freestream conditions. In addition, parameter studies to determine the sensitivity of the method to assumptions regarding velocity profile shape, shear stress relations, and initial conditions should be carried out as part of any evaluation.

It is also recommended that several improvements be made to the procedure in order to increase the applicability and accuracy of the method. Thus, the method may be readily adapted to wings, provided the three-dimensional pressure distribution is used and provided cross-flow effects in the jet layer remain small. Improved accuracy should result by employing Coles-type velocity profiles in the boundary-layer zone in place of the present power law profiles. The method may also be extended to flows with thick jets, such as for over the wing blowing, by retaining terms in the momentum equation of order δ/R. Finally, the introduction of compressibility effects into the inviscid and jet layer computational procedures should permit the eventual treatment flows with variable density and possibly with shocks.

Appendix

The following expressions have been derived for the coefficients appearing in Eq. (6):

$$A_1 = -u_e\delta_1$$

$$B_1 = \frac{u_m\delta_1}{(2n+1)(n+1)}$$

$$D_1 = \frac{nu_m^2}{(2n+1)(n+1)}$$

$$E_1 = u_m^2\delta_1\left[\frac{1}{(n+1)^2} - \frac{2}{(2n+1)^2}\right]$$

$$C_1 = F_1 = G_1 = H_1 = 0$$

$$A_2 = -u_e\delta/2$$

$$B_2 = \frac{u_m\delta_1}{(2n+1)(n+1)}\left[1 - \left(\frac{1}{2}\right)^{2n+1}\right]$$

$$D_2 = -\frac{nu_m^2}{(2n+1)(n+1)}\left[1 - \left(\frac{1}{2}\right)^{2n+1}\right]$$

$$E_2 = \frac{u_m^2\delta_1}{(n+1)(2n+1)}\left\{\left(\frac{1}{2}\right)^{2n+1} ln2 + \frac{\left[1 - \left(\frac{1}{2}\right)^{2n+1}\right](2n^2-1)}{(n+1)(2n+1)}\right\}$$

$$C_2 + F_2 = G_2 = H_2 = 0$$

$$A_3 = -u_e$$

$$B_3 = u_m$$

$$C_3 = D_3 = E_3 = F_3 = G_3 = H_3 = 0$$

$$A_4 = -u_e(\delta_3 - \delta_2)$$

$$B_4 = (\delta_3 - \delta_2)[2u_m(1 - F_{31}) - 2(u_m - u_w)(F_{31} - F_{32}) - u_w(1 - F_{31})] + (u_m - u_w)\left[\frac{\delta_1}{n+1} + \delta_2 - \delta_1\right]$$

$$C_4 = (\delta_3 - \delta_2)[2u_mF_{31} - 2(u_m - u_w)F_{32} - u_wF_{31}]$$

$$D_4 = -\frac{n}{n+1}u_m(u_m - u_w)$$

$$E_4 = -\frac{u_m\delta_1}{(n+1)^2}(u_m - u_w)$$

$$F_4 = (u_m - u_w)[u_m F_{31} + (u_m - u_w)(F_{31} - F_{32})]$$

$$G_4 = (u_m - u_w)[u_m(1 - F_{31}) - (u_m - u_w)(F_{31} - F_{32})]$$

$$H_4 = 0$$

$$A_5 = -(1 - \bar{\eta}_3)u_e(\delta_3 - \delta_2)$$

$$B_5 = (\delta_3 - \delta_2)\left[2u_m(1 - \bar{\eta}_3 - F_{\frac{3}{2}1}) - 2(u_m - u_w) \times (F_{\frac{3}{2}1} - F_{\frac{3}{2}2}) - \left(\frac{u_w + u_m}{2}\right)(1 - \bar{\eta}_3 - F_{\frac{3}{2}1})\right] + \left(\frac{u_m - u_w}{2}\right)\left[\frac{\delta_1}{n+1} + \delta_2 - \delta_1\right]$$

$$C_5 = (\delta_3 - \delta_2)\left[2u_m F_{\frac{3}{2}1} - 2(u_m - u_w)F_{\frac{3}{2}2} - \left(\frac{u_m + u_w}{2}\right)F_{\frac{3}{2}1}\right]$$

$$D_5 = -\left(\frac{n}{n+1}\right)u_m\left(\frac{u_m - u_w}{2}\right)$$

$$E_5 = -\frac{\delta_1}{(n+1)^2}u_m\left(\frac{u_m - u_w}{2}\right)$$

$$F_5 = \left(\frac{u_m - u_w}{2}\right)\left[u_m(\bar{\eta}_3 + 2F_{\frac{3}{2}1}) - (u_m - u_w)(2F_{\frac{3}{2}2} - F_{\frac{3}{2}1})\right]$$

$$G_5 = \left(\frac{u_m - u_w}{2}\right)\left[u_m(1 - \bar{\eta}_3 - 2F_{\frac{3}{2}1}) - (u_m - u_w)(F_{\frac{3}{2}1} - 2F_{\frac{3}{2}2})\right]$$

$$H_5 = 0$$

$$A_6 = -(y_{1/2} - \delta_3)[u_e F_{41} + 2(u_e - u_w)(F_{41} + F_{42})]$$

$$B_6 = -(u_e - u_w)\left[\frac{\delta_1}{n+1} + \delta_2 - \delta_1 + (\delta_3 - \delta_2)(1 - F_{31})\right]$$

$$C_6 = (y_{1/2} - \delta_3)[u_e F_{41} + 2(u_e - u_w)F_{42}] - (\delta_3 - \delta_2)(u_e - u_w)F_{31}$$

$$D_6 = \left(\frac{n}{n+1}\right)u_m(u_e - u_w)$$

$$E_6 = \frac{u_m\delta_1}{(n+1)^2}(u_e - u_w)$$

$$F_6 = -(u_m - u_w)(u_e - u_w)F_{31}$$

$$G_6 = -(u_e - u_w)[u_e(1 - F_{41}) + (u_e - u_w)(1 - F_{42}) + (u_m - u_w)(1 - F_{31})]$$

$$H_6 = -(u_e - u_w)[u_e F_{41} + (u_e - u_w)F_{42}]$$

$$A_7 = -(y_{1/2} - \delta_3)\left[\left(u_e + \frac{u_e - u_w}{2}\right)F_{\frac{4}{2}1} - \left(\frac{u_e - u_w}{2}\right) + 2(u_e - u_w)(F_{\frac{4}{2}1} + F_{\frac{4}{2}2})\right]$$

$$B_7 = -\left(\frac{u_e - u_w}{2}\right)\left[\frac{\delta_1}{n+1} + \delta_2 - \delta_1 + (\delta_3 - \delta_2)(1 - F_{31})\right]$$

$$C_7 = (y_{1/2} - \delta_3)\left[\left(u_e + \frac{u_e - u_w}{2}\right)F_{\frac{4}{2}1} + 2(u_e - u_w)F_{\frac{4}{2}2}\right] - (\delta_3 - \delta_2)F_{31}\left(\frac{u_e - u_w}{2}\right)$$

$$D_7 = \left(\frac{n}{n+1}\right)u_m\left(\frac{u_e - u_w}{2}\right)$$

$$E_7 = \frac{u_m\delta_1}{(n+1)^2}\left(\frac{u_e - u_w}{2}\right)$$

$$F_7 = -F_{31}(u_m - u_w)\left(\frac{u_e - u_w}{2}\right)$$

$$G_7 = -(u_e - u_w)\left\{\left[u_e + \left(\frac{u_e - u_w}{2}\right)\right](1 - F_{\frac{4}{2}1}) + (u_e - u_w)(1 - F_{\frac{4}{2}2})\right\} - (u_m - u_w)(1 - F_{31})\left(\frac{u_e - u_w}{2}\right)$$

$$H_7 = \left(\frac{u_e - u_w}{2}\right)\left[\left(u_e + \frac{u_e - u_w}{2}\right)(1 - 2F_{\frac{4}{2}1}) + (u_e - u_w)\left(\frac{1}{2} - 2F_{\frac{4}{2}2}\right)\right]$$

$$F_{31} = \int_0^1 f(\eta_3)d\eta_3$$

$$F_{32} = \int_0^1 f^2(\eta_3)d\eta_3$$

$$F_{\frac{3}{2}1} = \int_{\bar{\eta}_3}^1 f(\eta_3)d\eta_3$$

$$F_{\frac{3}{2}2} = \int_{\bar{\eta}_3}^1 f^2(\eta_3)d\eta_3$$

$$F_{41} = \int_0^\infty g(\eta_4)d\eta_4$$

$$F_{42} = \int_0^\infty g^2(\eta_4)d\eta_4$$

$$F_{\frac{4}{2}1} = \int_0^1 g(\eta_4)d\eta_4$$

$$F_{\frac{4}{2}2} = \int_0^1 g^2(\eta_4)d\eta_4$$

References

[1]Levinsky, E. S. and Yeh, T. T., "Analytical and Experimental Investigation of Circulation Control by Means of a Turbulent Coanda Jet," CR-2114, Sept. 1972, NASA.

[2]Dixon, C. J., "Lift and Control Augmentation by Spanwise Blowing over Trailing Edge Flaps and Control Surfaces," AIAA Paper 72-781, Los Angeles, Calif., 1972.

[3]Thomas, F., "Untersuchungen uber die Erhöhung des Auftriebs von Tragflügeln Mittels Grenzschichtbeeinflussung durch Ausblasen," *Zeitshcrift Flugwissenschaften*, Vol. 10, 1962, Heft 2.

[4]Carriere, P. and Eichelbrenner, E. A., "Theory of Flow Reattachment by a Tangential Jet Discharging Against a Strong Adverse Pressure Gradient," *Boundary Layer and Flow Control*, edited by G. V. Lachmann, Pergamon Press, New York, 1961, Vol I, pp. 209-231.

[5]Cebeci, T., Mosinskis, G. J., and Smith, A. M. O., "Calculation of Separation Points in Incompressible Turbulent Flows," *Journal of Aircraft*, Vol. 9, No. 9, Sept. 1972, pp. 618-624.

[6]Bhateley, I. C. and McWhirter, J. W., "Development of Theoretical Method for Two-Dimensional Multi-Element Airfoil Analysis and Design, Part I: Viscous Flow Analysis Method," AFFDL-TR-72-96, Pt. I, Aug. 1972, Air Force Flight Dynamics Lab., Wright-Patterson Air Force Base, Ohio.

[7]Spence, D. A., "The Lift on a Thin Aerofoil with a Blown Flap," RAE TN Aero 2450, May 1956, Royal Aircraft Establishment, Farnborough, England.

[8]Herold, A. C., "A Two-Dimensional, Interative Solution for the Jet Flap," CR-2190, Feb. 1973, NASA.

[9]Dvorak, F. A., "Calculation of Turbulent Boundary Layers and Wall Jets over Curved Surfaces," *AIAA Journal*, Vol. 11, No. 4, April 1973, pp. 517-524.

[10]Goradia, S. H. and Colwell, G. T., "Parametric Study of a Two-Dimensional Turbulent Wall Jet in a Moving Stream with Arbitrary Pressure Gradient," *AIAA Journal*, Vol. 9, No. 11, Nov. 1971, pp. 2156-2165.

[11]Kacker, S. C. and Whitelaw, J. H., "Some Properties of the Two-Dimensional Turbulent Wall Jet in a Moving Stream," *Journal of Applied Mechanics*, Vol. 35, No. 4, Dec. 1968, pp. 641-651.

[12]Schlichting, H., *Boundary Layer Theory*, McGraw-Hill, New York, 1968, pp. 590-609.

[13]Bangert, L. H., "The Turbulent Wall Jet with an Initial Boundary Layer," AIAA Paper 71-612, Palo Alto, Calif., 1971.

[14]Gartshore, I. S. and Newman, B. C., "The Turbulent Wall Jet in an Arbitrary Pressure Gradient," *The Aeronautical Quarterly*, Vol. XX, Pt. I, Feb. 1969, pp. 25-56.

[15]Coles, D., *Proceedings, Computation of Turbulent Boundary Layers—1968, AFOSP-IFP-Stanford Conference*, Vol. II, Aug. 18-25, 1968, pp. 1-46.

[16]Lawford, J. A. and Foster, D. N., "Low Speed Wind Tunnel Tests on a Wing Section with Plain Leading- and Trailing-Edge Flaps Having Boundary Layer Control by Blowing," RAE TR 69078, April 1969, Royal Aircraft Establishment, Farnborough, England.

JANUARY 1975 J. AIRCRAFT VOL. 12, NO. 1

Thin-Airfoil Theory of an Ejector-Flapped Wing Section

Henry W. Woolard*
U.S. Air Force Flight Dynamics Laboratory, Wright-Patterson Air Force Base, Ohio

A theoretical analysis of the aerodynamics of a thin ejector-flapped wing section (augmentor wing) is presented. The idealized external and internal (ejector) flowfields and their approximate interfacing are treated. The linearized external flowfield analysis is an extension of Spence's method for jet-flapped airfoils. Summary curves of the section lift and pitching-moment characteristics and their relation to the ejector characteristics are presented. Fourier coefficients are tabulated for use in calculating airfoil surface pressure distributions and other flowfield details. The idealized lift performance of an ejector-flapped wing relative to a jet augmented flapped wing is compared and the ejector-flapped wing is found to be substantially superior at low forward-speed ratios. The relation of the present work to that of Y. Y. Chan is noted.

Nomenclature

A = cross-sectional area
b_f = ejector-flap span
c = airfoil chord ($c = 1$ in external aerodynamics analysis)
c_f = flap chord
c_h = flap hinge-moment coefficient about flap leading edge, based on c_f^2 (positive, trailing-edge down)
c_j = primary-jet installed momentum coefficient, $\rho U_j^2 \bar{h}_j / q_\infty c$
$\hat{c}_j$ = primary-jet uninstalled momentum coefficient, $\rho \hat{U}_j^2 h_j / q_\infty c$
c_j^* = primary-jet test momentum coefficient, $\rho U_j h_j \hat{U}_j / q_\infty c$
c_J = ejector exit-flow momentum coefficient, $\rho U_E^2 h_E / q_\infty c$
c_l = lift coefficient
c_{m_0} = airfoil nose-up pitching-moment coefficient about the leading edge
c_{nf} = flap normal-force coefficient
c_p = pressure coefficient, $(p - p_\infty)/q_\infty$; for small perturbations, $-2u'/U_\infty$
c_Q = thin-airfoil suction coefficient, $Q/U_\infty c$
c_Q = ejector net suction coefficient, $(U_s - U_\infty) h_s / U_\infty c$
$\check{c}_Q$ = ejector gross suction coefficient, $U_s h_s / U_\infty c$; $(\check{c}_Q = c_Q + \bar{h}_s/c)$
c_T = ejection net-thrust coefficient, $(\rho U_E^2 h_E - \rho U_s U_\infty h_s / q_\infty c$
$\hat{c}_t$ = primary-jet uninstalled net thrust coefficient, $\rho \hat{U}_j (\hat{U}_j - U_\infty) h_j / q_\infty c$
E_n = Fourier coefficients for trailing jet-sheet vorticity distribution
$f(x)$ = nondimensional vorticity distribution along the airfoil, $f(x) = \gamma(x)/U_\infty c$
$g'(x)$ = nondimensional vorticity distribution along the trailing jet sheet, $g'(x) = \gamma(x)/U_\infty c$
h_e, h_E = heights at ejector diffuser inlet and exit, respectively
$\bar{h}_j$ = mean height of ejector primary-jet nozzle, A_j/b_f
h_s = mean height of ejector secondary flow passage at primary-jet, A_s/b_f
p = static pressure
P = total pressure
q_∞ = freestream dynamic pressure, $(\rho/2) U_\infty^2$
Q = two-dimensional ideal flow sink strength
u = local velocity parallel to freestream
u' = perturbation velocity, $(u - U_\infty)$
U = mean local axial velocity within the ejector (except U_∞)
$\hat{U}_j$ = primary-jet uninstalled isentropic velocity, $[(2/\rho)(P_j - p_\infty)]^{1/2}$
$\tilde{U}_x$ = $U_x/\hat{U}_j$, where $x = j, s, E$, etc.
U_∞ = freestream velocity
$\tilde{U}_\infty$ = forward-speed parameter, $U_\infty/\hat{U}_j$
w = downwash velocity, positive downward
x, y = rectangular coordinates, see Fig. 2
x_s = chordwise location of sink on airfoil of unit chord
X = $[1 - (1 - x)^{1/2}]/[1 + (1 - x)^{1/2}]$
α = angle of attack
γ = vorticity, $d\Gamma/dx$ or $(u'_u - u'_l)$
Γ = total circulation
δ_f = trailing-edge flap deflection angle, positive for trailing-edge down
ϵ = local slope of airfoil surface
θ, φ = polar coordinates defined by Eq. (27)
λ = $4/c_J$
ξ, η = dummy variables
ρ = density
σ = $\sigma = 1$ for an upper-surface sink, $\sigma = -1$ for a lower-surface sink
Ω_D = ejector diffuser area ratio, A_E/A_e

Subscripts and Superscripts

Ω_j = ejector injection area ratio, A_s/A_j
a = denotes the airfoil
J = denotes the trailing jet sheet
T = denotes the trailing streamline for an unblown airfoil
$'$ = denotes differentiation with respect to the indicated argument (except u')
D = denotes the diffuser
e = ejector station e, see Fig. 6

Presented as Paper 74-187 at the AIAA 12th Aerospace Sciences Meeting, Washington, D.C., January 30-February 1, 1974; submitted February 12, 1974; revision received July 22, 1974.

Index categories: Aircraft Aerodynamics (including Component Aerodynamics); Subsonic and Transonic Flow; Jets, Wakes, and Viscid-Inviscid Flow Interactions.

*Aerospace Engineer, Flight Control Division, Control Criteria Branch (FGC). Associate Fellow AIAA.